Detection of free radicals produced from the reaction of cytochrome *P*-450 with linoleic acid hydroperoxide

Cristina ROTA*[1], David P. BARR†, Martha V. MARTIN‡, F. Peter GUENGERICH‡, Aldo TOMASI* and Ronald P. MASON†

*Department of Biomedical Sciences, University of Modena, via Campi 276, 41100 Modena, Italy, †National Institute of Environmental Health Sciences, National Institutes of Health, Research Triangle Park, NC 27709, U.S.A., and ‡Department of Biochemistry and Center of Molecular Toxicology, Vanderbilt University School of Medicine, Nashville, TN 37232–0146, U.S.A.

The ESR spin-trapping technique was employed to investigate the reaction of rabbit cytochrome *P*-450 1A2 (P450) with linoleic acid hydroperoxide. This system was compared with chemical systems where $FeSO_4$ or $FeCl_3$ was used in place of P450. The spin trap 5,5′-dimethyl-1-pyrroline *N*-oxide (DMPO) was employed to detect and identify radical species. The DMPO adducts of hydroxyl, $O_2^{-\bullet}$, peroxyl, methyl and acyl radicals were detected in the P450 system. The reaction did not require NADPH–cytochrome *P*-450 reductase or NADPH. The same DMPO–radical adducts were detected in the $FeSO_4$ system. Only DMPO–$^{\bullet}$OH radical adduct and carbon-centred radical adducts were detected in the $FeCl_3$ system. Peroxyl radical production was completely O_2-dependent. We propose that polyunsaturated fatty acids are initially reduced to form alkoxyl radicals, which then undergo intramolecular rearrangement to form epoxyalkyl radicals. Each epoxyalkyl radical reacts with O_2, forming a peroxyl radical. Subsequent unimolecular decomposition of this peroxyl radical eliminates $O_2^{-\bullet}$ radical.

INTRODUCTION

Lipid hydroperoxides are derived from the oxidation of polyunsaturated fatty acids. The decomposition of lipid hydroperoxides has been studied over several years because, in biological systems, lipid-derived free radicals are known to cause damage to biomembranes, proteins and other biomolecules [1–3]. Fatty acid hydroperoxides are known for their ability to bleach cytochrome *P*-450; in other words, they destroy the haem group of this haemoprotein [4,5]. Free radicals are also involved in these reactions [6–9].

In a widely accepted breakdown mechanism, one-electron reduction of fatty acid hydroperoxide produces alkoxyl radicals [3,10–12]. It has been proposed that these alkoxyl radicals cyclize to their adjacent double bonds, forming epoxy allyl carbon-centred free radicals. The carbon-centred radicals react with O_2, forming peroxyl radicals [12,13]. These carbon-centred radicals have been described in the decomposition of lipid hydroperoxide catalysed by haematin, ram seminal vesicles [11] and lipoxygenase [12,14,15].

The first studies that provided evidence for alkoxyl radical intermediates from fatty acid hydroperoxides were based on product analysis [10,14,16]. 5,5′-Dimethyl-1-pyrroline *N*-oxide (DMPO)–alkoxyl and –acyl radical adducts have been detected after toluene extraction [17]. The spin trapping of secondary alkoxyl radicals in aqueous systems has proven difficult, apparently because of their rapid cyclization. However, product analysis and spin-trapping investigations have demonstrated that fatty acid alkoxyl radicals undergo intramolecular epoxidation [10,14,15,18], β-scission [15,18,19] and intermolecular reactions [20].

Linoleic acid is one of the most abundant polyunsaturated fatty acids in biological membranes [21]. For this reason the study of 13-hydroperoxide octadecadienoic acid (13-HPODE), one of the two hydroperoxides derived from oxidation of this fatty acid, is of interest. In the present study we have investigated the mechanism of 13-HPODE degradation by cytochrome *P*-450 1A2 (P450) and have compared it with chemical systems in which free radicals were produced from the breakdown of 13-HPODE by Fe^{3+} or Fe^{2+} ions.

There has been disagreement as to how the peroxide O–O bond is cleaved by the P450, i.e. heterolytically or homolytically [22–27]. Recently, Barr et al. [28] demonstrated that P450 produces radicals from cumene hydroperoxide via the homolytic mechanism. In this study we have investigated the reaction of P450 with 13-HPODE with the purpose of clarifying the mechanism of radical production and characterizing the structures of fatty acid hydroperoxide-derived free radicals.

MATERIALS AND METHODS

Chemicals

P450 was purified from rabbit hepatic microsomes (5,6-benzoflavone-treated rabbits) [29,30]. Soya-bean lipoxidase type IV (450000 units/mg of protein), linoleic acid sodium salt and deferoxamine mesylate (DFO) were purchased from Sigma (St. Louis, MO, U.S.A.). DMPO was purchased from Aldrich (Milwaukee, WI, U.S.A.); it was vacuum-distilled twice at room temperature. Glucose oxidase (250 units/mg), catalase (65000 units/mg) and superoxide dismutase (SOD; 5000 units/mg) were obtained from Boehringer-Mannheim (Indianapolis, IN, U.S.A.). All reagents and buffers were prepared in deionized water and treated with Chelex 100 (Bio-Rad, Hercules, CA, U.S.A.).

ESR spin-trapping experiments

The ESR spectra were recorded using a Bruker ECS-106 spectrometer operating at 9.77 GHz with a modulation frequency of 50 kHz and TM_{110} cavity. The reactions were initiated by the addition of P450 or iron. For the experiments shown in Figure 6, glucose (20 mM) and glucose oxidase (143 μg/ml) were added to the reaction mixture 2 min before the addition of $FeSO_4$ to produce anaerobic conditions; catalase (50 μg/ml) was also

Abbreviations used: P450, cytochrome *P*-450 1A2; DFO, deferoxamine mesylate; 13-HPODE, linoleic acid hydroperoxide; SOD, superoxide dismutase; DMPO, 5,5′-dimethyl-1-pyrroline *N*-oxide.

[1] To whom correspondence should be addressed at NIH/NIEHS, MD F0-02, P.O. Box 12233, Research Triangle Park, NC 27709, U.S.A.

added. The reactions were all performed in Chelex-treated 50 mM phosphate buffer, pH 7.4; when required, 50 μM DFO was added to inhibit possible reactions catalysed from traces of metals. Since light may enhance the breakdown of 13-HPODE, all experiments were performed in the dark.

Computer simulation

Computer simulations were performed using a program that is available to the public through the Internet (HTTP://lmb.niehs.nih.gov/LBM/). The details of this program have been described elsewhere [31].

Synthesis of 13-HPODE

13-HPODE was prepared by the method of Gardner [32] with the following modifications: use of 2 mM linoleic acid sodium salt as substrate and soya-bean lipoxidase type IV (5 mg). The reaction was performed in 100 ml of Chelex-treated 100 mM borate buffer, pH 9, with the addition of 50 μM DFO (60 min on ice under oxygen, with constant stirring). The reaction mixture was extracted with 2 vol. of ethyl acetate, and the lipid layer washed twice with 1 vol. of water. Reverse-phase semi-preparative HPLC was used to purify the 13-HPODE. The method used was a modification of the method of Henke et al. [33]. Separation of 13-HPODE from unchanged metabolites was obtained by elution with a mobile phase that consisted of 75 parts of methanol, 25 parts of water and 0.01 part of acetic acid by volume; flow rate was 5.8 ml/min. Concentration of 13-HPODE and elimination of water were achieved by forming an azeotrope with acetonitrile. Purified 13-HPODE was stored at -70 °C in 300 μl aliquots. The concentration was estimated at A_{234} using an absorption coefficient of 25.6 $cm^{-1} \cdot mM^{-1}$ [34].

P450 destruction

Destruction of P450 by 13-HPODE was monitored spectrophotometrically as the decrease in A_{418}. Spectra were recorded on an Aminco DW-2000 spectrophotometer equipped with a double beam.

RESULTS

The ferric form of purified rabbit P450 exists primarily in the low-spin configuration with a maximum absorbance in the Soret

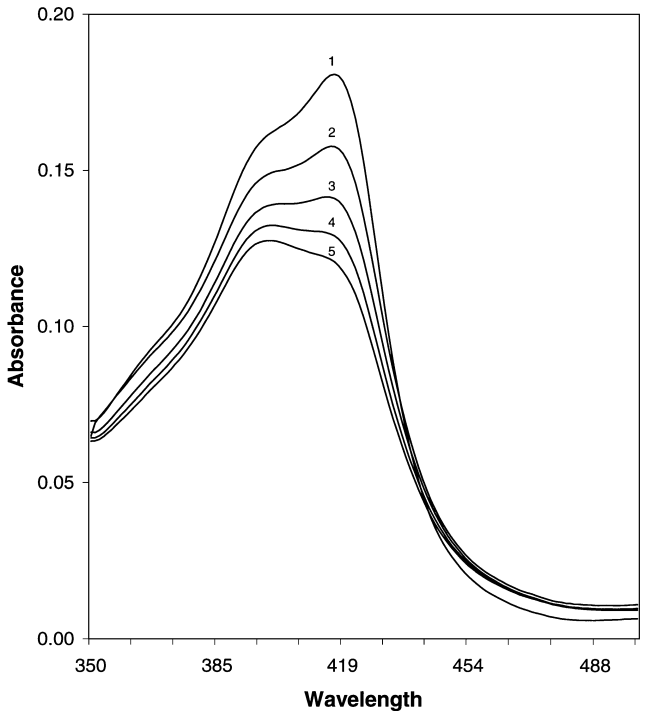

Figure 1 Time course of P450 destruction induced by 13-HPODE

P450 was diluted to 3 μM with 50 mM phosphate buffer, pH 7.4, containing 30% glycerol. Spectra were recorded every 40 s for a total of five scans. After recording of the initial spectrum (see also ref. [30]), 600 μM 13-HPODE was added directly to the sample cuvette. Spectra were recorded versus the same buffer as reference for the initial spectrum, and against a 600 μM 13-HPODE solution for the following scans.

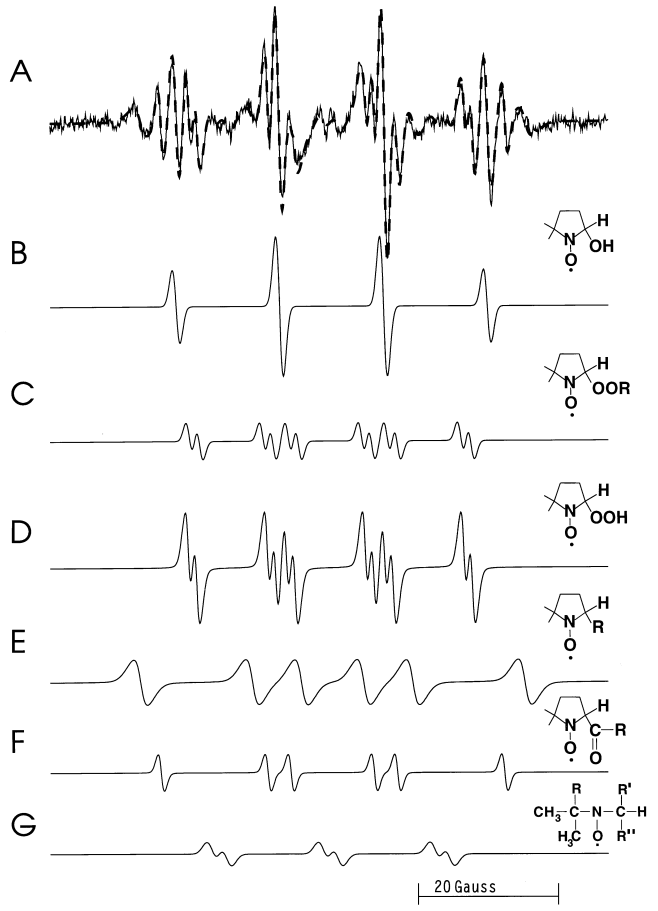

Figure 2 Computer simulation and deconvolution of ESR spectrum obtained from the reaction mixture containing P450, 13-HPODE and DMPO

A is the computer simulation (dashed line) superimposed on the experimental spectrum obtained using 3 μM P450, 1.2 mM 13-HPODE, 50 μM DFO and 300 mM DMPO. B–G are the individual simulations of each species in the composite spectrum. The hyperfine coupling constants of each species are provided in the text. B is the simulated spectrum for DMPO–$^{\bullet}$OH (line width, 0.56 G; line shape, 0% Lorentzian, 100% Gaussian; mol ratio, 0.21). C is the simulated spectrum for DMPO–$^{\bullet}$OOR (line width, 0.53 G; line shape, 0% Lorentzian, 100% Gaussian; mol ratio, 0.06). D is the simulated spectrum for DMPO–$^{\bullet}$OOH (line width, 0.58 G; line shape, 44% Lorentzian, 56% Gaussian; mol ratio, 0.30). E is the simulated spectrum for DMPO–$^{\bullet}$R (line width, 1.31 G; line shape, 56% Lorentzian, 44% Gaussian; mol ratio, 0.26). F is the simulated spectrum for DMPO–$^{\bullet}$C(O)R (line width, 0.51 G; line shape, 33% Lorentzian, 67% Gaussian; mol ratio, 0.10). G is the simulated spectrum for the ring-opened DMPO$^{\bullet}$ radical (line width, 0.84 G; line shape, 0% Lorentzian, 100% Gaussian; mol ratio, 0.07). Spectrometer conditions were: modulation amplitude, 0.5 G; microwave power, 20 mW; time constant, 0.164 s; scan time, 168 s; scan range, 80 G receiver gain, 4×10^5. 1G = 10^{-4}T.

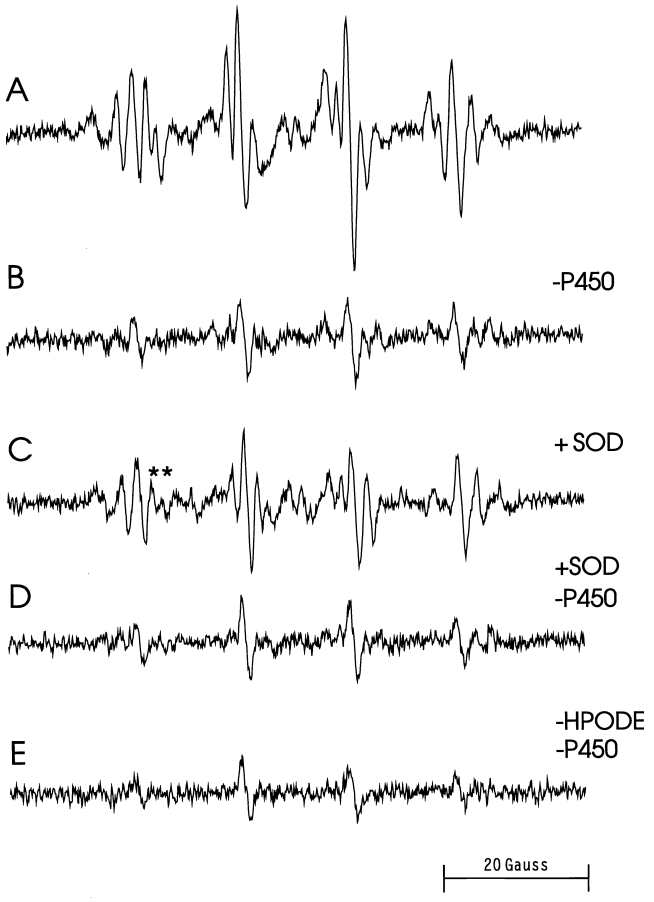

Figure 3 ESR spectra of DMPO–radical adducts produced by the reaction of P450 and 13-HPODE

A is the ESR spectrum obtained from a reaction mixture containing 3 μM P450, 1.2 mM 13-HPODE, 50 μM DFO and 300 mM DMPO (the same spectrum as Figure 2A). B is the spectrum obtained using the conditions of spectrum A except P450 was omitted. C is the spectrum of the complete system with the addition of SOD (50 μg/ml). D is the spectrum obtained using the conditions of spectrum C but with the omission of P450. E is the spectrum obtained using buffer and DMPO alone.

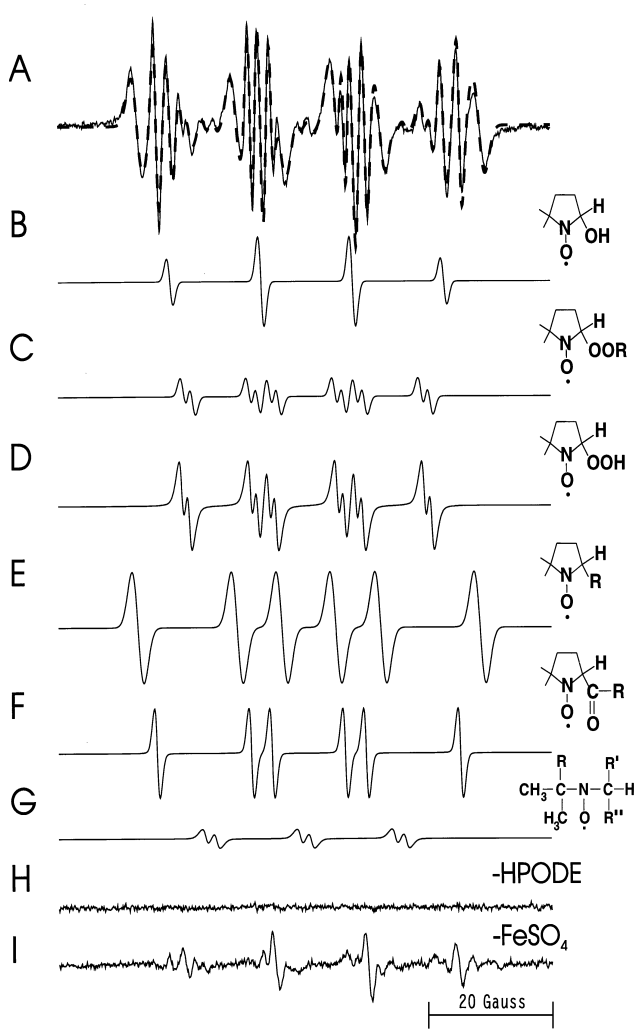

Figure 4 Computer simulation and deconvolution of the ESR spectrum obtained from the reaction mixture containing $FeSO_4$, 13-HPODE and DMPO

A is the computer simulation (dashed line) superimposed on the experimental spectrum obtained using 1 mM $FeSO_4$, 1.2 mM 13-HPODE and 600 mM DMPO. B–G are the individual simulations of each species in the composite spectrum. The hyperfine values of each species are provided in the text. B is the simulated spectrum for DMPO–$^{\bullet}$OH (line width, 0.52 G; line shape, 0% Lorentzian, 100% Gaussian; mol ratio, 0.16). C is the simulated spectrum for DMPO–$^{\bullet}$OOR (line width, 0.54 G; line shape, 0% Lorentzian, 100% Gaussian; mol ratio, 0.04). D is the simulated spectrum for DMPO–$^{\bullet}$OOH (line width, 0.68 G; line shape, 68% Lorentzian, 32% Gaussian; mol ratio, 0.16). E is the simulated spectrum for DMPO–$^{\bullet}$R (line width, 0.96 G; line shape, 0% Lorentzian, 100% Gaussian; mol ratio, 0.39). F is the simulated spectrum for DMPO–$^{\bullet}$C(O)R (line width, 0.50 G; line shape, 30% Lorentzian, 70% Gaussian; mol ratio, 0.21). G is the simulated spectrum for the ring-opened DMPO$^{\bullet}$ radical (line width, 0.76 G; line shape, 53% Lorentzian, 47% Gaussian; mol ratio, 0.04). H is the spectrum obtained using the conditions of spectrum A with omission of 13-HPODE. I is the spectrum obtained using the conditions of spectrum A with omission of $FeSO_4$, and addition of 50 μM DFO. Spectrometer conditions were as described in Figure 2. 1 G = 10^{-4} T.

region at 418 nm [30]. 13-HPODE is known to bleach P450 absorption at 418 nm [4,5,7]. We have repeated this degradation of the P450 by 13-HPODE. After recording the absolute absorption spectrum of a solution of P450, 13-HPODE was added directly to the cuvette; A_{418} gradually decreased, reaching a minimum 120 s after the addition of 13-HPODE (Figure 1).

The ESR spin-trapping technique was employed to investigate free-radical production during the reaction between P450 and 13-HPODE. When 13-HPODE was incubated with P450 under aerobic conditions in the presence of DMPO and DFO, a mixture of six radical adducts was detected (Figure 2). The computer simulation used to obtain the hyperfine coupling constants was superimposed on the experimental spectrum (Figure 2, spectrum A). On the basis of the hyperfine coupling constants, the radical adducts were assigned as follows: DMPO–$^{\bullet}$OH ($a^{N} = 14.96$ G and $a_{\beta}^{H} = 14.72$ G), DMPO–$^{\bullet}$OOH ($a^{N} = 14.11$ G, $a_{\beta}^{H} = 11.34$ G, and $a_{\gamma}^{H} = 1.22$ G), DMPO–$^{\bullet}$OOR ($a^{N} = 14.21$ G, $a_{\beta}^{H} = 10.54$ G, and $a_{\gamma}^{H} = 1.41$ G), DMPO–$^{\bullet}$R ($a^{N} = 16.01$ G and $a_{\beta}^{H} = 23.07$ G), DMPO–$^{\bullet}$C(O)R ($a^{N} = 15.31$ G and $a_{\beta}^{H} = 18.64$ G), and one radical species probably derived from the opening of the DMPO ring ($a^{N} = 16.02$ G and $a_{\beta}^{H} = 1.94$ G); this spin-trap decomposition product is similar to one previously detected [35]. The hyperfine coupling constants were consistent with previously reported values for these adducts [36–39]. When P450 was omitted, only a weak ESR signal was detected (Figure 3, spectrum B). This spectrum was mainly that of DMPO–$^{\bullet}$OH, which is obtained from DMPO alone (Figure 3, spectrum E). This result demonstrated that the detected radical adducts came from the reaction of P450 with 13-HPODE, and not from 13-HPODE itself. SOD (50 μg/ml) only inhibited the

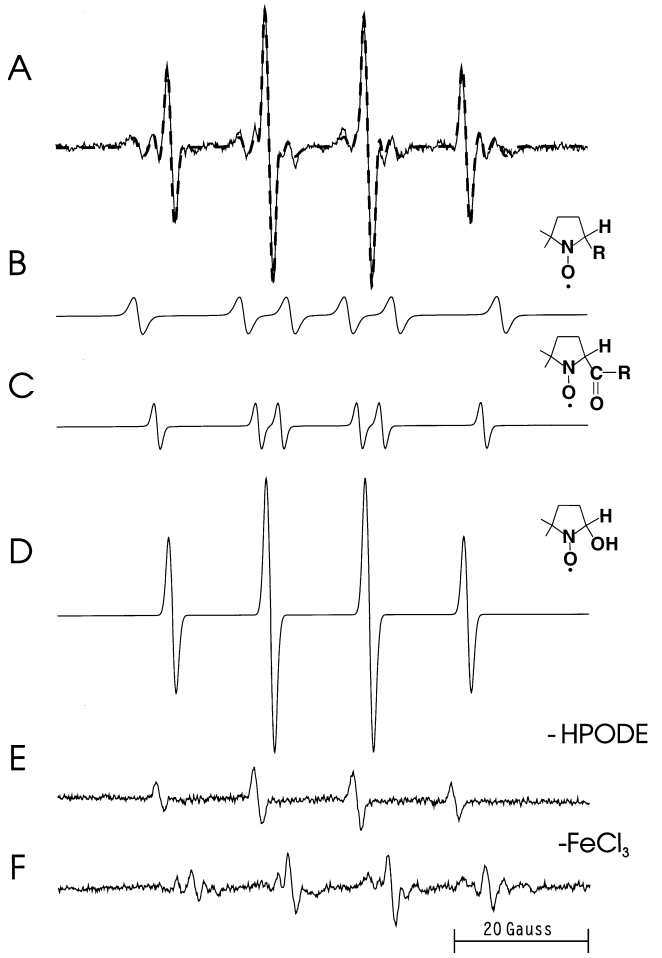

Figure 5 Computer simulation and deconvolution of the ESR spectrum obtained from the reaction mixture containing $FeCl_3$, 13-HPODE and DMPO

A is the computer simulation (dashed line) superimposed on the experimental spectrum obtained using 1 mM $FeCl_3$, 1.2 mM 13-HPODE and 600 mM DMPO. B–D are the individual simulations of each species in the composite spectrum. The hyperfine coupling constants of each species are provided in the text. B is the simulated spectrum for DMPO–$^{\bullet}$R (line width, 0.85 G; line shape, 48% Lorentzian, 52% Gaussian; mol ratio, 0.22). C is the simulated spectrum for DMPO–$^{\bullet}$C(O)R (line width, 0.50 G; line shape, 27% Lorentzian, 73% Gaussian; mol ratio, 0.11). D is the simulated spectrum for DMPO–$^{\bullet}$OH (line width, 0.54 G; line shape, 0% Lorentzian, 100% Gaussian; mol ratio, 0.67). E is the spectrum obtained using the conditions of spectrum A with omission of 13-HPODE. F is the spectrum obtained using the conditions of spectrum A with omission of $FeCl_3$ and addition of 50 μM DFO. Spectrometer conditions were as described in Figure 2. 1 G = 10^{-4} T.

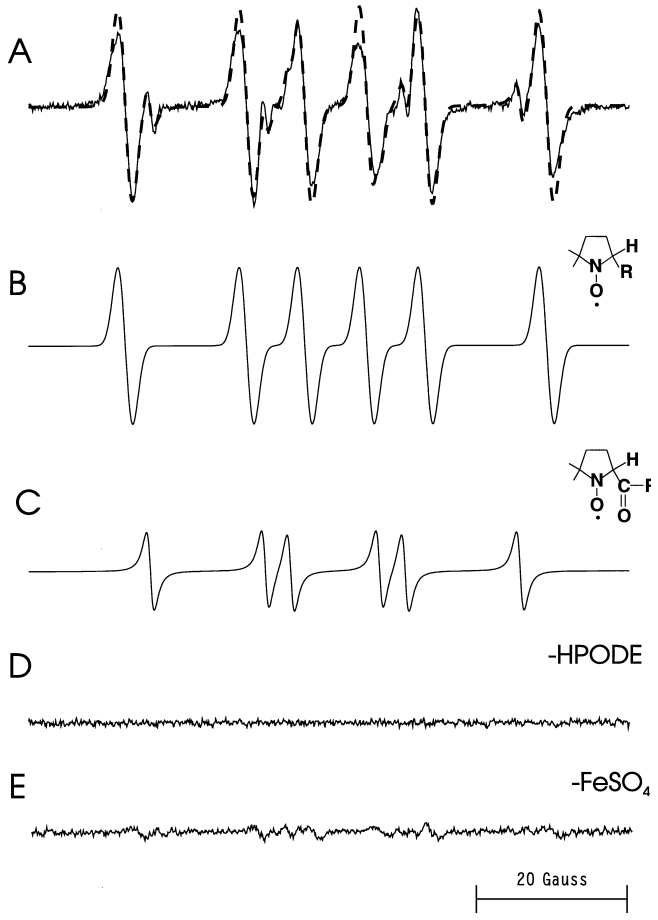

Figure 6 computer simulation and deconvolution of the ESR spectrum obtained from the reaction of $FeSO_4$ with 13-HPODE under anaerobic conditions

A is the computer simulation (dashed line) superimposed on the experimental spectrum obtained from a reaction mixture containing 1 mM $FeSO_4$, 1.2 mM 13-HPODE, 600 mM DMPO, 20 mM glucose, 143 μg/ml glucose oxidase and 50 μg/ml catalase. B–C are the individual simulations of each species in the composite spectrum. The hyperfine coupling constants of each species are provided in the text. B is the simulated spectrum for DMPO–$^{\bullet}$R (line width, 0.97 G; line shape, 0% Lorentzian, 100% Gaussian; mol ratio, 0.83). C is the simulated spectrum for DMPO–$^{\bullet}$C(O)R (line width, 0.89 G; line shape, 100% Lorentzian, 0% Gaussian; mol ratio, 0.17). D is the spectrum obtained using the conditions of spectrum A with omission of 13-HPODE. E is the spectrum obtained using the conditions of spectrum A with omission of $FeSO_4$ and addition of 50 μM DFO. Spectrometer conditions were as described in Figure 2. 1 G = 10^{-4} T.

formation of the DMPO–$O_2^{-\bullet}$ radical adduct. The resulting ESR spectrum still contained the spectroscopically similar peroxyl radical adduct (see asterisks in Figure 3, spectrum C). This radical adduct had hyperfine coupling constants of $a^N = 14.20$ G, $a_\beta^H = 10.65$ G and $a_\gamma^H = 1.40$ G, which are consistent with previously reported values for the peroxyl radical adduct [36]. The same spectrum was recorded when SOD (100 μg/ml) was added (results not shown).

We detected the same radical species using $FeSO_4$ instead of P450. The computer simulation used to obtain the hyperfine coupling constants gave an excellent fit to the experimental spectrum (Figure 4, spectrum A). On the basis of the hyperfine coupling constants, the radical adducts were assigned as follows: DMPO–$^{\bullet}$OH ($a^N = 14.92$ G and $a_\beta^H = 14.73$ G), DMPO–$^{\bullet}$OOH ($a^N = 14.16$ G, $a_\beta^H = 11.15$ G, and $a_\gamma^H = 1.24$ G), DMPO–$^{\bullet}$OOR ($a^N = 14.02$ G, $a_\beta^H = 10.65$ G, and $a_\gamma^H = 1.39$ G), DMPO–$^{\bullet}$R ($a^N = 16.09$ G and $a_\beta^H = 23.40$ G), DMPO–$^{\bullet}$C(O)R ($a^N = 15.31$ G and $a_\beta^H = 18.71$ G) and ring-opened DMPO radical ($a^N = 15.44$ G and $a_\beta^H = 1.79$ G). The hyperfine values were consistent with previously reported values for these adducts [36,37,40]. The addition of SOD (100 μg/ml) to the $FeSO_4$ system resulted in a spectrum in which the peroxyl radical adduct was clearly apparent (results not shown). The addition of DFO, a well-known Fe^{3+}-chelating agent, had effect only on the DMPO–$^{\bullet}$OH radical adduct, which became weaker (results not shown). This demonstrated that, in part, this radical came from Fe^{3+} ions. DMPO–$^{\bullet}$OH production is known to occur through the Fe^{3+}-catalysed nucleophilic addition of water [41,42].

13-HPODE was also allowed to react with $FeCl_3$. In this system we detected DMPO–hydroxyl radical and carbon-centred

Table 1 Hyperfine coupling constants of DMPO radical adducts (Figures 2–6)

	Hyperfine coupling constants (G)										
	P450 system			$FeSO_4$ system			$FeCl_3$ system		Literature values		
Radicals	a^N	a^H_β	a^H_γ	a^N	a^H_β	a^H_γ	a^N	a^H_β	a^N	a^H_β	Reference
$O_2^{-\bullet}$	14.11	11.34	1.22	14.16	11.15	1.24			14.18	11.31	[38]
									14.20	11.10	[40]
$^\bullet$OOR	14.21	10.54	1.41	14.02	10.65	1.39			14.20	10.64	[36]
$^\bullet$R	16.01	23.07		16.09	23.40		15.86	22.97	16.20	23.39	[36]
									15.90	23.00	[39]
$^\bullet$C(O)R	15.31	18.64		15.31	18.71		15.28	18.69	15.36	18.78	[36]
$^\bullet$OH	14.96	14.72		14.92	14.73		14.97	14.58	14.99	14.58	[37]

radicals. The computer simulation used to obtain the hyperfine coupling constants was superimposed on the experimental spectrum (Figure 5, spectrum A). On the basis of the hyperfine coupling constants, the radical adducts were assigned as follows: DMPO–$^\bullet$OH ($a^N = 14.97$ G and $a^H_\beta = 14.58$ G), DMPO–$^\bullet$R ($a^N = 15.86$ G and $a^H_\beta = 22.97$ G), and DMPO–$^\bullet$C(O)R ($a^N = 15.28$ G and $a^H_\beta = 18.69$ G). The hyperfine coupling constants were consistent with previously reported values for these adducts [36,37,39]. The addition of DFO to the system had no effect on radical adduct production (results not shown).

SOD had no effect on the DMPO–hydroxyl radical adduct in the $FeCl_3$ system (results not shown). The addition of catalase or glucose had no effect on the P450 or $FeSO_4$ systems. The addition of catalase to the $FeCl_3$ system had a weak inhibitory effect on $^\bullet$OH production (results not shown).

To obtain strict anaerobic conditions, we added glucose and glucose oxidase to the systems. To avoid possible effects from H_2O_2 production, a small amount of catalase was also added. Under these conditions, we did not detect any peroxyl or $O_2^{-\bullet}$ radical adducts. In the anaerobic P450 system, we detected only a weak spectrum of one radical species (results not shown). On the basis of the hyperfine coupling constants, the radical adduct was assigned as DMPO–$^\bullet$R ($a^N = 16.18$ G and $a^H_\beta = 23.31$). In the $FeSO_4$ system, two carbon-centred radical adducts were detected as shown in Figure 6. We assigned these radical adducts as DMPO–$^\bullet$R ($a^N = 16.10$ G and $a^H_\beta = 23.91$ G) and DMPO–$^\bullet$C(O)R ($a^N = 15.29$ G and $a^H_\beta = 18.71$ G). The hyperfine coupling constants were consistent with previously published values for these adducts [36,43]. The addition of DFO to the system has some inhibitory effect on the acyl radical adduct (results not shown). A summary of the hyperfine coupling constant values for the DMPO–radical adducts is provided in Table 1.

DISCUSSION

Sufficient evidence has been reported to support the idea that P450 can catalyse both homolytic and heterolytic peroxide bond cleavage [44–47]. The conclusion of these studies was that the ratio of heterolytic to homolytic cleavage depends on the P450 enzyme used. The heterolytic cleavage of the peroxide O–O bond involved formation of peroxyl radicals that is completely independent of O_2 as shown below.

$$\text{P450-Fe}^{(III)} + \text{ROOH} \xrightarrow{\text{Heterolytic}} \text{P450}^{\bullet+}(\text{Fe}^{IV}=\text{O}) + \text{ROH} \quad (1)$$

$$\text{P450}^{\bullet+}(\text{Fe}^{IV}=\text{O}) + \text{ROOH} \rightarrow \text{P450}\,(\text{Fe}^{IV}=\text{O}) + \text{ROO}^\bullet \quad (2)$$

In the homolytic cleavage, the first radical produced is an alkoxyl radical (reaction 3)

$$\text{P450-Fe}^{(III)} + \text{ROOH} \xrightarrow{\text{Homolytic}} \text{P450}\,(\text{Fe}^{IV}=\text{O}) + \text{RO}^\bullet + \text{H}^+ \quad (3)$$

The mechanism of peroxyl radical production can be indirect

$$\text{RO}^\bullet \xrightarrow{\beta\text{-scission}} \text{R}^\bullet + \text{R}=\text{O} \quad (4)$$

$$\text{R}^\bullet + \text{O}_2 \rightarrow \text{ROO}^\bullet \quad (5)$$

or by direct oxidation of the hydroperoxide by Fe^{3+} ion or P450.

$$\text{Fe}^{(III)} + \text{ROOH} \rightarrow \text{Fe}^{(II)} + \text{ROO}^\bullet \quad (6)$$

In the $FeCl_3$ system we have detected only hydroxyl radical and very weak carbon-centred radicals. We have not found evidence for the production of the peroxyl radical that would be formed in reaction 6. Presumably $FeSO_4$ catalysed only the homolytic cleavage of the hydroperoxide as shown below.

$$\text{Fe}^{(II)} + \text{ROOH} \rightarrow \text{Fe}^{(III)} + \text{RO}^\bullet + {}^-\text{OH} \quad (7)$$

The production of peroxyl radicals may follow the mechanism illustrated in reactions 4–5. Since, in our systems, the production of peroxyl radicals disappeared completely in the absence of O_2, and because we have detected the same radical species on reaction of 13-HPODE with P450 or $FeSO_4$, we can conclude that P450, in this case, catalysed the reductive homolytic cleavage of the O–O bond of the lipid hydroperoxide. It should be noted that the hyperfine coupling constants for DMPO–primary alkoxyl radical adducts are similar to those of DMPO–peroxyl adducts [42]. Thus the adduct we are assigning to the peroxyl radical adduct might be an alkoxyl adduct. In either case, the radical adduct would be derived from a peroxyl radical formed from molecular O_2 and would not change our mechanistic conclusions.

Our results demonstrate that $O_2^{-\bullet}$, hydroxyl, peroxyl and carbon-centred DMPO–radical adducts were produced in both the P450 and the $FeSO_4$ systems. The addition of DFO to samples where no catalyst was added had a remarkable effect. In the presence of DFO, we detected only a very weak signal (Figure 4, spectrum I and Figure 5, spectrum F). In the absence of the chelating agent, the spectrum was stronger. This effect was more evident under anaerobic conditions (results not shown).

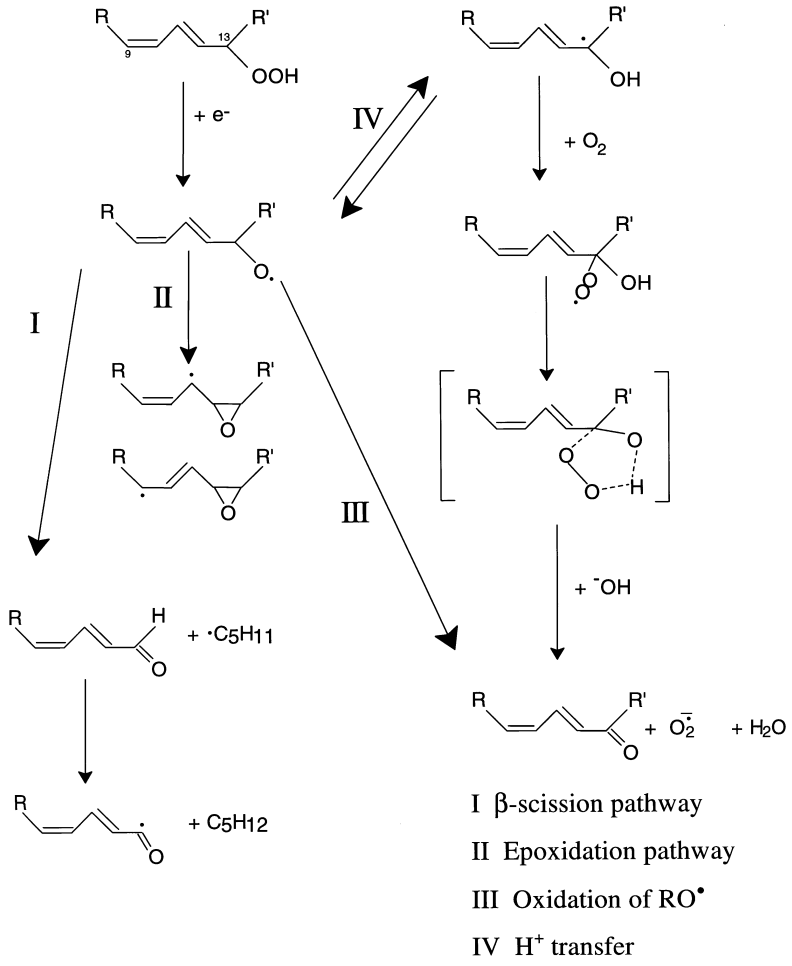

Scheme 1 Proposed mechanism for P450-catalysed metabolism of 13-HPODE

This means that, with the relatively high concentration of spin trap used in this study, we have detected radicals that arise from the reaction of 13-HPODE with contaminating Fe^{3+} ions. This reaction was of great importance in the control systems, but did not show a significant effect in the systems where the catalyst was added.

Some of the carbon-centred radicals detected in our system were recently detected in a system in which linoleic acid was allowed to react with lipoxidase in the presence of the spin trap α-(4-pyridyl-1-oxide)-*N*-*t*-butylnitrone. The radical species were identified using combined HPLC/ESR and tandem mass spectroscopy [15].

We propose the following reaction mechanism to explain our results. The one-electron reductive homolytic decomposition of the lipid hydroperoxide by P450 results in the formation of alkoxyl radicals (Scheme 1) [36,48]. Epoxy allylic radicals are formed by intramolecular rearrangement of fatty acid alkoxyl radicals (Scheme 1, reaction II) [10–12]. β-Scission of the alkoxyl radical (Scheme 1, reaction I) generates aldehyde and alkyl radical (e.g. *n*-pentyl radical) [19,20]. Immediate hydrogen abstraction from aldehyde by the concomitantly generated *n*-pentyl radical could then yield an acyl radical and pentane [17]. The reactive fatty acid alkoxyl radical undergoes an apparent hydrogen transfer that forms a hydroxyalkyl radical (Scheme 1, reaction IV) [49]. Under aerobic conditions, molecular O_2 adds to this radical to form a peroxyl radical [36].

The detected peroxyl radical could come either from the reaction of O_2 with the pentyl radical product of the β-scission pathway or the hydroxyalkyl radical derived from hydrogen transfer. Unfortunately no spectral distinction among the various types of DMPO–peroxyl radical adducts exists. Either case is consistent with our mechanistic conclusion (see Scheme 1).

The hydroxyalkyl peroxyl radical forms a cyclic five-membered transition state which eliminates $O_2^{-\bullet}$ radical, forming an oxo fatty acid (13-oxo-octadecadienoic acid). 13-Oxo-octadecadienoic acid could also be formed by direct oxidation of the corresponding alkoxyl radical (Scheme 1, reaction III) [50]. $O_2^{-\bullet}$ production via this chemistry has been reported [51,52]. This work suggests the possibility that $O_2^{-\bullet}$ and other free radicals could be formed from fatty acid hydroperoxides in biological systems by P450. Fatty acid alkoxyl radicals are considered too reactive to diffuse a significant distance from the site of generation [53]. $O_2^{-\bullet}$ may diffuse further than the alkoxyl radical. Protonated $O_2^{-\bullet}$ reacts with fatty acids, propagating lipid peroxidation [54]. Also, peroxyl radical formation could initiate lipid peroxidation. On the other hand, the high reactivity of the fatty acid alkoxyl radicals would make them good candidates for the reactive species responsible for the haem degradation that occurs during

the reaction of P450 with lipid hydroperoxides (Figure 1) [6–9]. The heterolytic reaction produces a two-electron oxidized form of P450 which hydroxylates substrates, probably without releasing free radicals [24,55,56], while the homolytic reaction produces diffusible free radicals.

On the basis of these results, we can conclude that the P450 homolytic mechanism degrades lipid hydroperoxides to highly reactive alkoxyl radicals, which react spontaneously to form both carbon-centred and $O_2^{-\cdot}$ radicals.

REFERENCES

1 O'Brien, P. J. (1988) in Cellular Antioxidant Defense Mechanisms, vol. 1, (Chow, C. K., ed.), pp. 73–87, CRC Press, Boca Raton, FL
2 Marnett, L. J. (1987) Carcinogenesis **8**, 1365–1373
3 Gardner, H. W. (1975) J. Agric. Food Chem. **23**, 129–136
4 Nerland, D. E., Iba, M. M. and Mannering, G. J. (1981) Mol. Pharmacol. **19**, 162–167
5 Iba, M. M. and Mannering, G. J. (1987) Biochem. Pharmacol. **36**, 1447–1455
6 Schaefer, W. H., Harris, T. M. and Guengerich, F. P. (1985) Biochemistry **24**, 3254–3263
7 Guengerich, F. P. (1986) Biochem. Biophys. Res. Commun. **138**, 193–198
8 Yao, K., Falick, A. M., Patel, N. and Correia, M. A. (1993) J. Biol. Chem. **268**, 59–65
9 Karuzina, I. I. and Archakov, A. I. (1994) Free Radical Biol. Med. **17**, 557–567
10 Dix, T. A. and Marnett, L. J. (1985) J. Biol. Chem. **260**, 5351–5357
11 Schreiber, J., Mason, R. P. and Eling, T. E. (1986) Arch. Biochem. Biophys. **251**, 17–24
12 Hughes, M. F., Chamulitrat, W., Mason, R. P. and Eling, T. E. (1989) Carcinogenesis **10**, 2075–2080
13 Dix, T. A., Fontana, R., Panthani, A. and Marnett, L. J. (1985) J. Biol. Chem. **260**, 5358–5365
14 Garssen, G. J., Veldink, G. A., Vliegenthart, J. F. G. and Boldingh, J. (1976) Eur. J. Biochem. **62**, 33–36
15 Iwahashi, H., Deterding, L. J., Parker, C. E., Mason, R. P. and Tomer, K. B. (1996) Free Radical Res. **25**, 255–274
16 Gardner, H. W., Weisleder, D. and Kleiman, R. (1978) Lipids **13**, 246–252
17 Davies, M. J. and Slater, T. F. (1987) Biochem. J. **245**, 167–173
18 Wilcox, A. L. and Marnett, L. J. (1993) Chem. Res. Toxicol. **6**, 413–416
19 Chamulitrat, W. and Mason, R. P. (1990) Arch. Biochem. Biophys. **282**, 65–69
20 Bors, W., Tait, D., Michel, C., Saran, M. and Erben-Russ, M. (1984) Isr. J. Chem. **24**, 17–24
21 Thompson, Jr., G. A. (1980) in The Regulation of Membrane Lipid Metabolism, (Thompson, Jr. G. A., ed.), pp. 1–17, CRC Press, Boca Raton, FL
22 Coon, M. J. and Blake, II, R. C. (1982) in Oxygenases and Oxygen Metabolism, (Nozaki, M., Yamamoto, S., Ishimura, T., Coon, M. J., Ernster, L. and Estabrook, R. W., eds.), pp. 485–495, Academic Press, New York
23 Weiss, R. H. and Estabrook, R. W. (1986) Arch. Biochem. Biophys. **251**, 348–360
24 Thompson, J. A. and Wand, M. D. (1985) J. Biol. Chem. **260**, 10637–10644
25 Vaz, A. D. N. and Coon, M. J. (1987) Proc. Natl. Acad. Sci. U.S.A. **84**, 1172–1176
26 Vaz, A. D. N. and Coon, M. J. (1990) Methods Enzymol. **186**, 278–282
27 Blake, II, R. C. and Coon, M. J. (1980) J. Biol. Chem. **255**, 4100–4111
28 Barr, D. P., Martin, M. V., Guengerich, F. P. and Mason, R. P. (1996) Chem. Res. Toxicol. **9**, 318–325
29 Alterman, M. A. and Dowgii, A. I. (1990) Biomed. Chromatogr. **4**, 221–222
30 Sandhu, P., Guo, Z., Baba, T., Martin, M. V., Tukey, R. H. and Guengerich, F. P. (1994) Arch. Biochem. Biophys. **309**, 168–177
31 Duling, D. R. (1994) J. Magn. Reson., Ser. B **104**, 105–110
32 Gardner, H. W. (1975) Lipids **10**, 248–252
33 Henke, D. C., Kouzan, S. and Eling, T. E. (1984) Anal. Biochem. **140**, 87–94
34 Lindstrom, T. D. and Aust, S. D. (1984) Arch. Biochem. Biophys. **233**, 80–87
35 Mottley, C. and Mason, R. P. (1989) in Biological Magnetic Resonance, vol. 8, (Berliner, L. J. and Reuben, J., eds.), pp. 489–546, Plenum Publishing Corp., New York
36 Chamulitrat, W., Hughes, M. F., Eling, T. E. and Mason, R. P. (1991) Arch. Biochem. Biophys. **290**, 153–159
37 Krainev, A. G., Williams, T. D. and Bigelow, D. J. (1996) J. Magn. Reson. **B111**, 272–280
38 Lloyd, R. V. and Mason, R. P. (1990) J. Biol. Chem. **265**, 16733–16736
39 Thornalley, P. J. and Stern, A. (1985) Biochem. Pharmacol. **34**, 1157–1164
40 Inoue, S. and Kawanishi, S. (1989) Biochem. Biophys. Res. Commun. **159**, 445–451
41 Makino, K., Hagiwara, T., Hagi, A., Nishi, M. and Murakami, A. (1990) Biochem. Biophys. Res. Commun. **172**, 1073–1080
42 Hanna, P. M., Chamulitrat, W. and Mason, R. P. (1992) Arch. Biochem. Biophys. **296**, 640–644
43 Buettner, G. R. and Oberley, L. W. (1979) FEBS Lett. **101**, 333–335
44 Shimizu, T., Murakami, Y. and Hatano, M. (1994) J. Biol. Chem. **269**, 13296–13304
45 Lee, W. A. and Bruice, T. C. (1985) J. Am. Chem. Soc. **107**, 513–514
46 Thompson, J. A. and Yumibe, N. P. (1989) Drug Metab. Rev. **20**, 365–378
47 Correia, M. A., Yao, K., Allentoff, A. J., Wrighton, S. A. and Thompson, J. A. (1995) Arch. Biochem. Biophys. **317**, 471–478
48 de Groot, J. J. M. C., Veldink, G. A., Vliegenthart, J. F. G., Boldingh, J., Wever, R. and van Gelder, B. F. (1975) Biochim. Biophys. Acta **377**, 71–79
49 Schuchmann, H. P. and von Sonntag, C. (1981) J. Photochem. **16**, 289–295
50 Labeque, R. and Marnett, L. J. (1987) J. Am. Chem. Soc. **109**, 2828–2829
51 Bothe, E., Schuchmann, M. N., Schulte-Frohlinde, D. and von Sonntag, C. (1978) Photochem. Photobiol. **28**, 639–644
52 Von Sonntag, C. (1989) in Free Radicals, Metal Ions and Biopolymers, (Beaumont, P. C., Deeble, D. J., Parsons, B. J. and Rice-Evans, C., eds.), pp. 73–84, Richelieu Press, London
53 Marnett, L. J. (1990) Adv. Exp. Med. Biol. **283**, 65–70
54 Bielski, B. H. J., Arudi, R. L. and Sutherland, M. W. (1983) J. Biol. Chem. **258**, 4759–4761
55 White, R. E. and Coon, M. J. (1980) Annu. Rev. Biochem. **49**, 315–356
56 Groves, J. T. and McClusky, G. A. (1976) J. Am. Chem. Soc. **98**, 859–861

Received 24 April 1997/11 July 1997; accepted 29 July 1997